Supporting Information

Hopkins et al. 10.1073/pnas.1120603109

SI Methods

1.1 Site Description. Litter and soil were collected at two free air CO_2 enrichment (FACE) experiments: Duke Forest FACE near Chapel Hill, North Carolina and Aspen FACE near Rhinelander, Wisconsin.

1.1.1 Duke FACE. The Duke FACE site, under forest cover since at least the 1940s, was burned and planted with loblolly pine (*Pinus taeda* L.) in 1983. Year-round CO_2 enrichment began in 1996 in three of four replicate plots. A prototype plot that served as the fourth replicate was additionally fumigated during the summers of 1994 and 1995 (1). There was no difference in C-isotope values of soils from the prototype plot and the values of the other three replicates. Loblolly pine dominates the aboveground biomass, with deciduous trees in the understory. The soils are low-fertility acidic clay loam Hapludalfs in the Enon Series, and they are poorly drained during wet periods. In 2005, the top 15 cm mineral soil had an average C content of 2.16 kg C m^{-2} (±0.15) and 2.10 kg C m^{-2} (±0.18) and $\delta^{13}C$ signature of −27.40 (±0.04) and −30.86 (±0.32) in ambient and elevated CO_2 plots, respectively (2). During the period of the FACE experiment, C was accumulating in the soils of both the ambient and elevated CO_2 plots because of recovery from disturbance (3).

1.1.2 Aspen FACE. The Aspen FACE site was agricultural land for at least 50 y up to 1972, when it was purchased by the US Department of Agriculture Forest Service and subsequently used for short-rotation forestry. The site was cleared and disked in 1996 and 1997, and Aspen clones (*Populus tremuloides* Michx.) were planted on one-half of each FACE plot in June of 1997. The remaining one-half of each plot was planted as one-quarter aspen with paper birch and one-quarter aspen with sugar maple, but for this experiment, only soils from the aspen monoculture were used. CO_2 fumigation began in 1998. Soils are Pandus clay loam: mixed, frigid, coarse loamy Alfic Haplorthods. Soil C contents increased linearly since the experiment began; in 2008, soil C was measured as 5.12 (±1.13) kg C m^{-2} in ambient CO_2 plots and 3.27 (±0.8) kg C m^{-2} in elevated CO_2 plots for the top 20 cm mineral soil, and soil C in elevated CO_2 plots was −31.1‰ in $\delta^{13}C$ (4).

1.2 FACE Experiments. Both experiments enriched CO_2 levels by 200 μmol mol^{-1} for the whole stands in each 30-m diameter treatment plot (1). The added CO_2 was derived from natural gas, which is very depleted in ^{13}C and ^{14}C relative to the background atmosphere. Fumigation gas was −43‰ in $\delta^{13}C$ and −1,000‰ in $\Delta^{14}C$ (5–7) compared with −8‰ in $\delta^{13}C$ and 40–110‰ in $\Delta^{14}C$ for the background atmosphere over the period of the FACE experiments (8, 9). The $\delta^{13}C$ of roots and leaves in elevated CO_2 plots confirms fixation of CO_2 with the expected isotopic admixture of fumigation gas and background air; root ingrowth cores measured root inputs as −39‰ at Duke, and roots picked from soil cores the year before our sampling (2008) measured root inputs as −39‰ at Aspen (10, 4, respectively).

1.3 Sampling Procedure. We sampled the top 0–15 cm mineral soil plus the overlying litter layer in each of the elevated and ambient CO_2 plots. We treated each FACE ring or experimental plot as the level of replication (Duke $n = 4$, Aspen $n = 3$).

Organic soil (litter layer) and mineral soils were collected from the Duke FACE on July 7, 2008. We sampled the litter layer by cutting a 100-cm^2 rectangle of all organic material found above the mineral soil surface. Mineral soils were sampled under the cleared area down to 15-cm depth using a 5-cm diameter slide hammer corer. Litter and mineral soils were collected at Aspen FACE on July 1, 2009. After surface litter removal, mineral soils were sampled with a 5-cm diameter impact corer in increments of 0–5 and then 5–15 cm.

1.4 Incubation Procedure. Soils were transported to the laboratory on ice and refrigerated before incubation. For both soils, rocks and roots were removed before incubation. For Duke soils, whole soil cores (minus roots) were placed in interior containers inside of 2-L Mason jars at field moisture content, and a subsample was taken after incubation to determine water content. For the Aspen site, mineral soils were additionally sieved to 4 mm, composited by ring, and then split using a cone and quarter method. About 140 g soil were used for incubation, with a subsample taken to determine soil moisture content before incubation. Because Aspen soils dried out during sieving, deionized water was added to soils after they were in incubation jars to return them to field moisture level.

Soils were kept at field moisture over the incubation period by high relative humidity inside of incubation jars. Soils were incubated continuously at site mean annual temperature, +10 °C, and +20 °C of warming, (Aspen: 5 °C, 15 °C, and 25 °C; Duke: 15 °C, 25 °C, and 25 °C; ±1 °C) for around 1 d before CO_2 fluxes were measured for the first time. Temperature treatments were monitored by a Stowaway Tidbit Temperature Logger (Onset Corporation) kept alongside soil samples during incubation and sampling. Soils were removed briefly from their temperature treatments for flux sampling (less than 1 h per sampling). Jars were removed from their temperature treatments and allowed to come to room temperature (24 °C) before CO_2 was removed from the jar.

1.5 CO_2 flux and isotope sampling. For soil CO_2 flux and isotope measurements, jars were capped with modified Mason jar lids fitted with stopcock-type sampling ports. Effective jar volume and potential leakage were checked by measuring the pressure change on expansion of the jar headspace into an evacuated known volume (11). At the beginning of the flux measurement period, jar headspace was purged with CO_2-free air at 1 L min^{-1} until the jar's volume had been completely purged at least three times before closing the jar and allowing CO_2 to accumulate in the headspace. Headspace CO_2 concentrations were measured in 2-mL syringe samples injected upstream of a CO_2 scrubber and air pump in line with a Licor 6252 Infrared Gas Analyzer (12). Fluxes were calculated as the CO_2 evolved for the effective jar volume for a given incubation time.

For each flux sampling period, we measured $\delta^{13}C$–CO_2 on air sampled directly from the jar headspace. Syringe samples were injected into He-filled vials for measurement of $\delta^{13}C$–CO_2 by continuous flow isotope ratio MS (Thermo Finnigan Gas Bench coupled to Delta Plus). $\delta^{13}C$ values are reported relative to the Pee Dee Belemnite standard.

For measurement of $\Delta^{14}C$–CO_2, jar headspace CO_2 was allowed to build up to 0.3–2.5% and then was collected using an evacuated container. CO_2 was purified cryogenically on a vacuum line and then reduced to graphite using the methods in the work by Xu et al. (13). Radiocarbon content of samples was measured at University of California at Irvine's W. M. Keck Carbon Cycle Accelerator Mass Spectrometer facility (14). Data are reported as $\Delta^{14}C$, the per mil difference in radiocarbon content relative to 95% of the activity of the oxalic acid I standard. $\Delta^{14}C$ was corrected for fractionation by normalizing to

−25‰ for samples from the ambient CO_2 plots (15). In enriched CO_2 atmospheres, the C-isotope signature of C fixed in photosynthesis does not just reflect C-isotope fractionation but rather, fractionation plus the mixing of different source gases (i.e., fumigation gas and atmosphere). Therefore, a different fractionation correction for $\Delta^{14}C$ must be used. Using the method from the work of Torn and Southon (16), we assumed that fractionation of C isotopes in photosynthesis was similar between CO_2 treatments, and we used the $\delta^{13}C$ values for ambient CO_2 soils to correct for mass-dependent fractionation in elevated CO_2 soils.

Error is reported as the SEM of samples from replicate plots, reflecting spatial heterogeneity among plots within the experiment sites. Error was propagated in isotopic mixing calculations using the procedure outlined in the work by Phillips and Gregg (17). Precision of all measurements was better than the SEM of replicate plots.

1.6 Postincubation. After incubation, Duke soils were sieved to 2 mm to remove any remaining rocks, and subsampled for soil moisture determination. No differences in soil moisture were found between temperature treatments. Both Duke and Aspen soils were dried at 60 °C and ground for analysis of bulk solid sample C and C-isotope content. Percent C and $\delta^{13}C$ were measured on aliquots of each sample using an NA 1500 NC elemental analyzer (Fisions Instruments) coupled to isotope ratio MS (as previously described).

1.7 Bomb ^{14}C Modeling. We used the record of Northern Hemisphere atmospheric ^{14}C content (9) and a steady-state, one-pool model of ^{14}C to determine the mean residence time of CO_2 respired during incubation (18). The model works on annual time steps, assuming that all C input to soil has the ^{14}C signature of that year's atmosphere. The decomposition rate, k, is inversely proportional to the turnover time of the modeled soil C pool, which is, in turn, closely related to that pool's mean residence time (assuming no lags in living tissue). If we consider the respired CO_2 to be coming from one homogeneous pool, k can be determined from $\Delta^{14}C$ of CO_2 respired. The model is solved independently for each treatment by iteratively adjusting k until model ^{14}C content equals the ^{14}C content of observation. The turnover time, estimated from $1/k$, represents the mean age of carbon being respired assuming a homogeneous C pool that contributes to microbial respiration. This mean age includes time spent by C in living tissues (e.g., roots or twigs) as well as the mean time for decomposition.

1.8 Isotopic Mixing Model. ***1.8.1 ^{14}C mixing model.*** We used an isotopic mixing model to take advantage of the decade-long FACE label. The principle of the model is similar to the principle of the ^{13}C mixing models used extensively at the FACE sites; we use the difference between ^{14}C content of preexisting soil C and FACE label C added since initiation of CO_2 fumigation. First, we calculate the ^{14}C signature of the FACE atmosphere (elevated CO_2 plots) for the mixture of background air and fossil-derived (−1,000‰) fumigation gas (Eq. **S1**):

$$\Delta^{14}C^{FACE} = \Delta^{14}C^{new}\left(\frac{[CO_2]_{atm}}{[CO_2]_{FACE}}\right) - 1000‰\left(\frac{[CO_2]_{FACE}-[CO_2]_{atm}}{[CO_2]_{FACE}}\right). \quad \textbf{[S1]}$$

We used the daytime CO_2 concentration records (7:00 AM to 7:00 PM) for experimental plots from the website of the two experiments (Duke, http://face.env.duke.edu; Aspen, http://aspenface.mtu.edu) to define the average CO_2 concentration of ambient and elevated CO_2 plots from the beginning of the CO_2 experiment to the year before the sampling. $[CO_2]_{atm}$, the atmospheric CO_2 content in ambient plots (and the background CO_2 endmember for the elevated CO_2 plots), is defined as the average (±SD) CO_2 concentration in ambient CO_2 plots (Duke, 379 ± 7; Aspen, 370 ± 18), and $[CO_2]_{FACE}$ is the measured CO_2 concentration in elevated CO_2 plots (Duke, 534 ± 16; Aspen, 531 ± 13). We assumed the $\Delta^{14}C^{new}$ was equal to the $\Delta^{14}C$ of the atmosphere in the year of sampling (Duke, 45‰; Aspen, 40‰), with a 5‰ error bar reflecting the seasonal cycle of Northern Hemisphere atmospheric $\Delta^{14}C$ (9).

Using the atmosphere's $\Delta^{14}C$ value as the new (<10 y) $\Delta^{14}C$ endmember assumes that all flux is coming from pools either <1 or >10 y old. However, the model is very insensitive to this endmember value because of the large isotopic difference between the CO_2 in FACE elevated CO_2 plots and ambient CO_2 plots. We tested this assumption by increasing $\Delta^{14}C^{new}$ by about 10‰ to simulate a mix of substrates with a 3 y mean residence time. This endmember changed the estimated proportion of flux from the pre-FACE pool by 0.01 (4% of original estimate).

Then, we partition fluxes from both ambient and elevated CO_2 plots into >10 and <10 y components by writing two mass balance equations for the flux (Eq. **S2**):

$$CO_2^{elev} = CO_2^{>10y} + CO_2^{<10y,elev} \quad \textbf{[S2]}$$

and (Eq. **S3**)

$$CO_2^{amb} = CO_2^{>10y} + CO_2^{<10y,amb}. \quad \textbf{[S3]}$$

We also wrote two equations for mass balance of the isotopes of flux (Eq. **S4**):

$$\Delta^{14}C^{elev}CO_2^{elev} = \Delta^{14}C^{>10y}CO_2^{>10y} + \Delta^{14}C^{FACE}CO_2^{<10y,elev} \quad \textbf{[S4]}$$

and (Eq. **S5**)

$$\Delta^{14}C^{amb}CO_2^{amb} = \Delta^{14}C^{>10y}CO_2^{>10y} + \Delta^{14}C^{new}CO_2^{<10y,amb}. \quad \textbf{[S5]}$$

If we assume the flux and $\Delta^{14}C$ content of the >10 y pool are the same for both CO_2 treatments (i.e., CO_2 fumigation had no effect on decomposition rates of previously existing soil C), then the system of equations can be solved for the fluxes from the <10 y pool of the elevated CO_2 treatment and ambient CO_2 treatment. In the original model (Fig. 3), we partitioned fluxes separately for each temperature treatment and site, deriving an independent $\Delta^{14}C^{>10\ y}$ for each incubation temperature.

1.8.2 Modified ^{14}C mixing model. We modified the CO_2 flux mixing model for the warming treatments by adding another CO_2 source pool to account for changes in the isotopic signature of respiration substrate with warming. First, we selected fluxes that represent the same amount of total C respired for each temperature treatment: 2.68% of soil carbon at Duke and 0.11% of soil carbon at Aspen. Second, we partitioned the fluxes from the elevated CO_2 treatment into FACE and pre-FACE C using the previous approach but with isotopic endmembers that did not change with temperature. In contrast to the original mixing model, where we determined $\Delta^{14}C^{>10y}$ separately for each temperature, we fixed $\Delta^{14}C^{>10y}$ to the value determined from the mean annual temperature control treatment. This change had little effect on the fraction of >10 y C contributing to overall flux across temperatures (Fig. 4).

From the increase in $\Delta^{14}C$ of CO_2 respired from the ambient CO_2 treatment with warming, we know that the increased flux was of an intermediate age: >3 y because the higher $\Delta^{14}C$ values indicate carbon fixed earlier in the bomb period but <10 y because of the proportion of pre-FACE carbon remains the same. We determined the age of additional substrates respired under warming using CO_2 fluxes from the ambient CO_2 treatment. As

previously, we assumed that the flux of >10 y C was the same for a given temperature between CO_2 treatments. In addition, we assumed that the contribution of C with a mean residence time of less than 1 y (i.e., C with the $\Delta^{14}C$ signature of that year's atmosphere) was constant across temperatures, and therefore, any additional flux with warming after subtracting out the increase in >10 y C was attributed to the warming-induced pool. We then used flux and isotopic mass balance equations to solve for the $\Delta^{14}C$ value of the warming-induced substrate, which was 7–13 y at Aspen and 9–12 y at Duke.

1.7.3 ^{13}C mixing model. We also used $\delta^{13}C$ of respiration fluxes and overall soil C stock to distinguish FACE C from pre-FACE C. We solve for fraction pre-FACE C (Eq. **S6**):

$$f_{pre-FACE} = \frac{\delta^{13}C_{elev} - \delta^{13}C_{new}}{\delta^{13}C_{amb} - \delta^{13}C_{new}}, \quad \text{[S6]}$$

where $\delta^{13}C_{elev}$ is the $\delta^{13}C$ signature of respired CO_2 (or soil C) from elevated CO_2 soils, $\delta^{13}C_{amb}$ is the $\delta^{13}C$ signature of respired CO_2 (or soil C) from ambient CO_2 soils, and $\delta^{13}C_{new}$ is the $\delta^{13}C$ signature of new photosynthate under CO_2 enrichment [Duke, −39‰ (10); Aspen, −39‰ (4)]. The model is very sensitive to the selection of the $\delta^{13}C_{new}$ endmember. The $\delta^{13}C$ of microbial respiration has been observed to change with both temperature and time in incubation (11, 19). A 2‰ change in the value of $\delta^{13}C_{new}$ results in a 20–50% change in the calculated proportion of pre-FACE C contributing to respiration. Instead, we report the error on the fraction of pre-FACE C in Table 2 as the SEM $\delta^{13}C$ values of mixing model components, which was propagated by the method in the work by Phillips and Gregg (17).

1.9 Cumulative Respiration Calculations. To correct for potential substrate limitation, we compared the same amount of C respired across temperatures (20). We chose a target amount of total C respired for which the isotopic signature could be consistently estimated across temperature treatments (2.68‰ of initial C respired for Duke and 0.11‰ of initial C respired for Aspen). We used periodic measurements of respiration and isotopes and linear interpolation between these measurements to determine cumulative amount of C respired and $\Delta^{14}C$ values when required.

1.9 Modeling of Data. All nonlinear model fits to data were performed using the Marquardt method in PROC NLIN of SAS version 9.2.

1.9.1 Modeling pool sizes and decay rates using fluxes over time. We fit a two-pool exponential decay model to fluxes from each temperature and CO_2 treatment combination in the Duke FACE soils, which was similar to the method described in the work by Paul et al. (21) (Eq. **S7**):

$$R_t = k_a C_a e^{-k_a t} + k_s(1 - C_a)e^{-k_s t}. \quad \text{[S7]}$$

Fluxes (R_t; units of μg C_{active} g C_{soil}^{-1} d^{-1}) were measured nine times over the course of the 373 d incubation for each of the four replicates, and these data were used to fit k_a (decay rate of active pool; units of d^{-1}), k_s (decay rate of slow pool; units of d^{-1}), and C_a (size of active pool; units of μg C_{active} g C_{soil}^{-1}).

No model was fit to Aspen data; there was no trend in fluxes over time (linear regression slope of fluxes against time was not significantly different from zero).

1.9.2 Modeling the temperature effect on partitioned fluxes. To describe the exponential dependence of flux on temperature, we fit an exponential model (11) to FACE label-partitioned fluxes [$R_{>10\ y}(T)$, $R_{<10\ y}(T)$] for each site and CO_2 treatment (Eq. **S8**):

$$R_{>10y}(T) = A_{>10y} e^{b_{>10y} T} \quad \text{[S8]}$$

and (Eq. **S9**)

$$R_{<10y}(T) = A_{<10y} e^{b_{<10y} T}. \quad \text{[S9]}$$

Temperature dependence can be quantified as (Eq. **S10**)

$$\frac{\partial R}{\partial T} = b * R, \quad \text{[S10]}$$

where b is the temperature sensitivity coefficient. We fit A and b separately for pre-FACE flux ($R_{>10\ y}$) and FACE flux ($R_{<10\ y}$). We report best fits and SE estimates from the nonlinear fit procedure.

1.11 Estimates of Decades-Old C. To determine how much of the overall 0–15 cm mineral soil C pool is vulnerable at both sites, we related the isotopic identity of fluxes to measurable C pools in the soil. Respiration fluxes consist of annually to decadally cycling C (Table 2), and therefore, we have to determine how much of the soil C stock is cycling on these timescales. We used different methods to assess the fraction of soil C stocks vulnerable to decomposition at Duke and Aspen sites because of differences in the data available and inherent soil C age structure between the two sites. Modeling C pools at both the sites using bomb radiocarbon incorporation is complicated by the relatively recent plowing history and young stand ages. Aspen is farther from steady state than Duke, because site disturbance is more recent.

1.11.1 Duke. Using the rate of addition of FACE-derived C into density and size fractions, the work by Lichter et al. (2) estimated the turnover time of pools in the Duke FACE soil. To relate these experimentally determined pools to the $\Delta^{14}C$ values of respiration, we measured the $\Delta^{14}C$ values of size and density fractions of 0–5 cm soils taken in July of 2008 from the Duke FACE experiment plots (Fig. 5). All fractions at the Duke FACE site are dominated by bomb-derived C (i.e., decadal or younger) with the exception of the >250-μm size fraction, which is dominated by prebomb C (i.e., millennial C). We estimated the size of the decadal soil carbon pool by subtracting carbon in the >250-μm size fraction for 0- to 15-cm depth from the total soil C stock at this depth.

This estimate is in accord with a bomb radiocarbon model for soil at the Duke site, consisting of 25% of C with a mean residence time of 3,700 y and 75% of C with a mean residence time of 25 y (22).

1.11.2 Aspen. Because of its recent disturbance history and young stand age, the Aspen site is far from steady state, which complicates turnover time calculations for soil C fractions. All size fractions experienced an increase in FACE-derived C over 4 y of the elevated CO_2 treatment, meaning that none of them are completely inert (23). However, stability of pools can be inferred from changes in the amount of pre-FACE C; the work by Hofmockel et al. (23) showed a significant decrease in the amount of pre-FACE C in the fine particulate organic matter (fPOM; 53–250 μm) and mineral-associated organic matter (MAOM; <53 μm) size fractions, but no change in the amount of pre-FACE C in the coarse particulate organic matter (>250 μm) fraction.

The work by Hofmockel et al. (23) also showed no time trend in total fPOM or MAOM stocks, suggesting that the pre-FACE components of C in the fPOM and MAOM fractions are indeed single homogeneous pools at steady state with respect to the total carbon. This finding means that we can assess the relative stability of these pools by dividing the stock by the flux to confirm that these pools are turning over on the order of decades (14 y for fPOM and 40 y for MAOM). If the pre-FACE fraction of C in coarse particulate organic matter soil size class represents

a stable pool, then we can subtract it from the total soil C to get an estimate of the maximum vulnerability of soil carbon at Aspen FACE for 0–15 cm soils: 94%.

Given the very low flux rates at Aspen FACE compared with Duke FACE, we can use another approach to estimate the minimum amount of decades-old C in the Aspen FACE soils. In this study, we partitioned CO_2 fluxes into FACE and pre-FACE components using the $\Delta^{14}C$ of respired CO_2. We also partitioned the bulk soil C stock into FACE and pre-FACE components using $\delta^{13}C$, showing that C predating the FACE treatment makes up 70% of the soil C pool at the 0- to 15-cm depth but only 30% of the flux.

Differences in the cycling rates of the fractions show that it is unlikely that all pre-FACE soil C is a homogeneous reservoir (23). We can assume that only a small part of total soil pre-FACE C is contributing to CO_2 flux and that the minimum turnover time for that component of pre-FACE C is 10 y (in keeping with the fact that this pool is >10 y old and ignoring any lags in plant tissue). We then multiply the measured flux of pre-FACE C by this turnover time to get an estimate for the smallest possible fraction of pre-FACE C that is contributing to respiration. Added to the stock of FACE C (which we assume is all decadal or younger), we estimate a minimum of 53% of the Aspen stock cycling on decades or shorter timescales.

1. Hendrey G, Ellsworth D, Lewin K, Nagy J (1999) A free-air enrichment system for exposing tall forest vegetation to elevated atmospheric CO2. *Glob Change Biol* 5: 293–309.
2. Lichter J, et al. (2008) Soil carbon sequestration in a pine forest after 9 years of atmospheric CO2 enrichment. *Glob Change Biol* 14:2910–2922.
3. Lichter J, et al. (2005) Soil carbon sequestration and turnover in a pine forest after six years of atmospheric CO2 enrichment. *Ecology* 86:1835–1847.
4. Talhelm AF, Pregitzer KS, Zak DR (2009) Species-specific responses to atmospheric carbon dioxide and tropospheric ozone mediate changes in soil carbon. *Ecol Lett* 12: 1219–1228.
5. Schlesinger WH, Lichter J (2001) Limited carbon storage in soil and litter of experimental forest plots under increased atmospheric CO2. *Nature* 411:466–469.
6. Pregitzer K, Loya W, Kubiske M, Zak D (2006) Soil respiration in northern forests exposed to elevated atmospheric carbon dioxide and ozone. *Oecologia* 148: 503–516.
7. Pataki D, et al. (2003) Tracing changes in ecosystem function under elevated carbon dioxide conditions. *Bioscience* 53:805–818.
8. Department of US Commerce NESRL (2009) *NOAA/ESRL/GMD CCGG Cooperative Air Sampling Network*. Available at http://www.esrl.noaa.gov/gmd/ccgg/flask.html. Accessed Sept. 9, 2011.
9. Levin I, et al. (2010) Observations and modelling of the global distribution and long-term trend of atmospheric 14CO(2). *Tellus B Chem Phys Meterol* 62:26–46.
10. Matamala R, Gonzàlez-Meler MA, Jastrow JD, Norby RJ, Schlesinger WH (2003) Impacts of fine root turnover on forest NPP and soil C sequestration potential. *Science* 302:1385–1387.
11. Czimczik CI, Trumbore SE (2007) Short-term controls on the age of micro-bial carbon sources in boreal forest soils. *J Geophys Res* 112: G03001.
12. Davidson E, Trumbore S (1995) Gas diffusivity and production of CO_2 in deep soils of the eastern Amazon. *Tellus B Chem Phys Meterol* 47:550–565.
13. Xu X, et al. (2007) Modifying a sealed tube zinc reduction method for preparation of ams graphite targets: Reducing background and attaining high precision. *Nucl Instrum Methods Phys Res B* 259:320–329.
14. Southon J, Santos G (2004) Ion source development at KCCAMS, University of California, Irvine. *Radiocarbon* 46:33–39.
15. Stuiver M, Polach H (1977) Reporting of C-14 data: Discussion. *Radiocarbon* 19: 355–363.
16. Torn M, Southon J (2001) A new C-13 correction for radiocarbon samples from elevated-CO2 experiments. *Radiocarbon* 43:691–694.
17. Phillips D, Gregg J (2001) Uncertainty in source partitioning using stable isotopes. *Oecologia* 127:171–179.
18. Trumbore S (2000) Age of soil organic matter and soil respiration: Radiocarbon constraints on belowground c dynamics. *Ecol Appl* 10:399–411.
19. Andrews J, Matamala R, Westover K, Schlesinger W (2000) Temperature effects on the diversity of soil heterotrophs and the delta c-13 of soil-respired CO_2. *Soil Biol Biochem* 32:699–706.
20. Conant RT, et al. (2008) Sensitivity of organic matter decomposition to warming varies with its quality. *Glob Change Biol* 14:868–877.
21. Paul EA, Morris SJ, Bohm S (2001) *Assessment Methods for Soil Carbon*, eds Lal R, Kimble JM, Follett RF, Stewart BA (Lewis Publishers), pp 193–206.
22. Harrison K, Broecker W, Bonani G (1993) A strategy for estimating the impact of CO2 fertilization on soil carbon storage. *Global Biogeochem Cycles* 7:69–80.
23. Hofmockel KS, Zak DR, Moran KK, Jastrow JD (2011) Changes in forest soil organic matter pools after a decade of elevated CO2 and O-3. *Soil Biol Biochem* 43: 1518–1527.

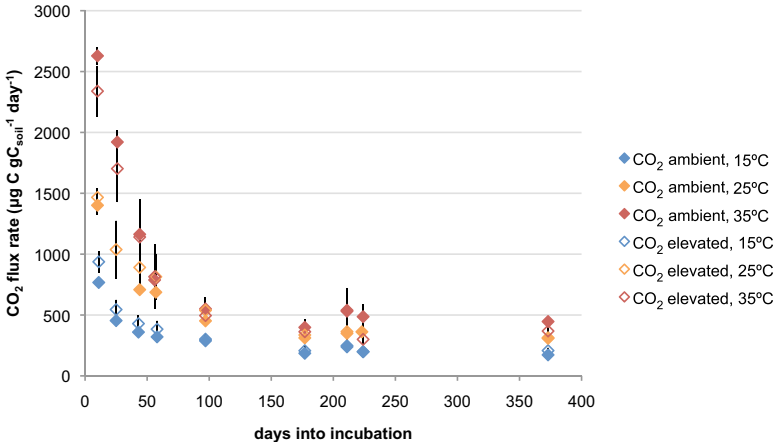

Fig. S1. CO_2 fluxes (micrograms C grams $soil^{-1}$ day^{-1}) over 373 d of incubation of Duke FACE soils. Solid symbols represent fluxes from the ambient CO_2 treatment, and open symbols represent fluxes from the elevated CO_2 treatment. Colors (blue, 15 °C; yellow, 25 °C; red, 35 °C) denote incubation temperature. Error bars represent the SEM of samples from four replicate plots for each treatment.

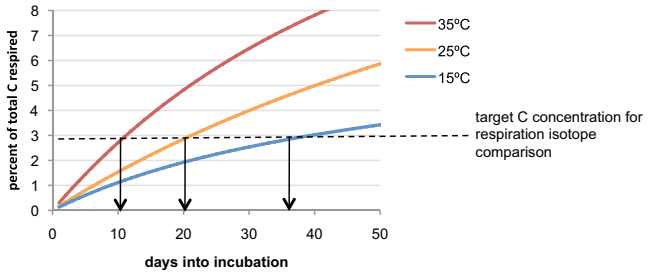

Fig. S2. Schematic representation of cumulative C respired (percent of initial soil C) by time into incubation. An equivalent amount of respired C was selected across temperature treatments, which is represented by the dashed line, and the isotopes of respiration were compared for the time period for which this C amount was respired.

Table S1. Two-pool model fit to flux time series data (Duke FACE only)

Ambient CO_2				Elevated CO_2			
Temperature (°C)	k_a	k_s	C_a	Temperature (°C)	k_a	k_s	C_a
15	17 (2)	0.09 (0.01)	18 (1)	15	16 (3)	0.09 (0.01)	25 (3)
25	11 (1)	0.14 (0.01)	44 (4)	25	7 (3)	0.14 (0.04)	64 (21)
35	13 (1)	0.20 (0.02)	90 (6)	35	11 (3)	0.17 (0.05)	86 (16)

k_a (year^{-1}) is the decay constant of the active pool, k_s (year^{-1}) is the decay constant of the slow pool, and C_a (milligrams C_{active} grams C_{soil}^{-1}) is the size of the active pool. Parameters were estimated for four replicate samples (±SEM).

Table S2. Soil carbon fractions (density and size separated) from Aspen and Duke FACE sites

	Aspen			Duke		
	C amount (g C m^{-2})			C amount (g C m^{-2})		
Fraction	Ambient CO_2	Elevated CO_2	$f_{>10\ y}$ by ^{13}C	Ambient CO_2	Elevated CO_2	$f_{>10\ y}$ by ^{13}C
Light fraction	530	515		1,431	1,697	0.44
>250 μm	480	460	0.50	473	562	0.90
53–250 μm	510	520	0.55	371	315	0.87
<53 μm	2,900	2,800	0.61	326	327	0.88

Data from the works by Hofmockel et al. (23) and Lichter et al. (3).